Structural Engineering and Mechanics, Vol. 9, No. 1 (2000) 51-68
DOI: http://dx.doi.org/10.12989/sem.2000.9.1.051

The inelastic buckling of varying thickness circular cylinders under external hydrostatic pressure

C.T.F. Ross†, A. Gill-Carson‡ and A.P.F. Little‡†

Department of Mechanical & Manufacturing Engineeering, University of Portsmouth, Portsmouth, Hants, PO1 3DJ, England

Abstract. The paper presents theoretical and experimental investigations on three varying thickness circular cylinders, which were tested to destruction under external hydrostatic pressure. The five buckling theories that were presented were based on inelastic shell instability. Three of these inelastic buckling theories adopted the finite element method and the other two theories were based on a modified version of the much simpler von Mises theory. Comparison between experiment and theory showed that one of the inelastic buckling theories that was based on the von Mises buckling pressure gave very good results while the two finite element solutions, obtained by dividing the theoretical elastic instability pressures by experimentally determined plastic knockdown factors gave poor results. The third finite element solution which was based on material and geometrical non-linearity gave excellent results. Electrical resistance strain gauges were used to monitor the collapse mechaisms and these revealed that collapse occurred in the regions of the highest values of hoop stress, where considerable deformation took place.

Key words: cylinders; varying thicknesses; buckling; external pressure; plasticity.

1. Introduction

Thin-walled circular cylinders with a stepped variation in wall thickness, appear in a number of different branches of engineering, including ocean engineering, agricultural engineering and aerospace engineering. In ocean engineering, such strucutures appear as the legs of off-shore structures and as underwater storage containers. In agricultural engineering, such structures appear as the fuselages of spacecraft.

Now under external hydrostatic pressure, such structures can fail through non-symmetric bifurcation buckling or shell instability (Ross 1990), at a pressure which might only be a small fraction of that to cause axisymmetric yield. The shell instability mode of failure is depicted in Fig. 1, where it can be seen that due to the compressive hoop stresses, the radial deformation pattern around the circumerence, is of a sinusoidal wave form.

If the unsupported meridional length of the vessel is small, then the cylinder can fail through axisymmetric collapse, as shown in Figs. 2 and 3.

In the case of axisymmetric deformation, the circumference at mid-bay becomes plastic and deforms axisymmetrically inwards. The result of this is to make the effects of axial pressure

† Professor
‡ Research Student
†‡ Senior Lecturer

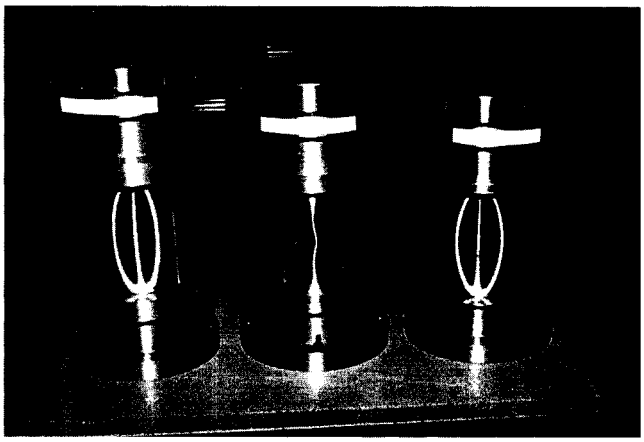

Fig. 1 Shell instability

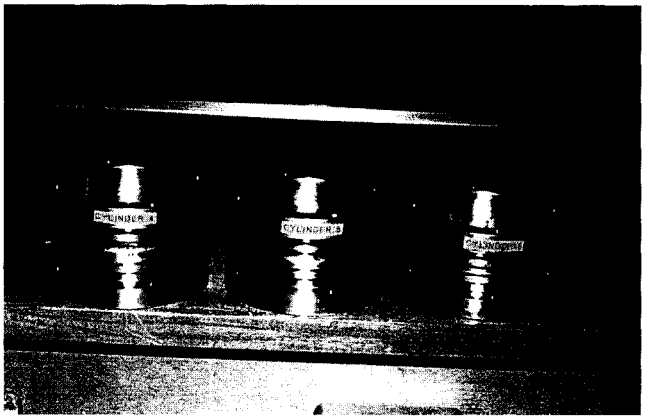

Fig. 2 Axisymmetric collapse

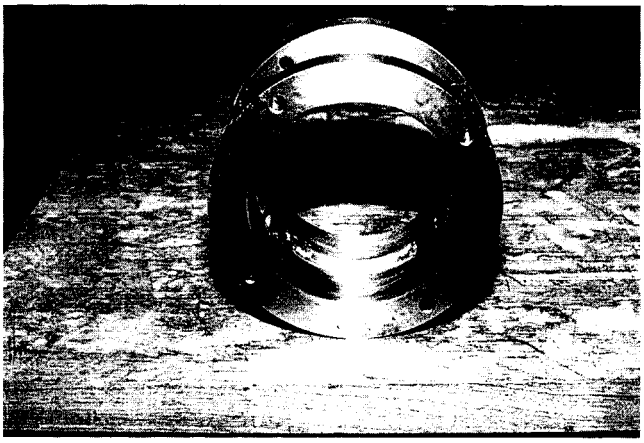

Fig. 3 Axisymmetric collapse (endview)

increasingly important, so that the mid-bay deforms even more rapidly inwards. Further increase in pressure causes the vessel to suffer from plastic axisymmetric collapse with two axisymmetric hogging hinges at the ends of the vessel and an axisymmetric sagging hinge at mid-bay.

In the case of a varying thickness circular cylinder, the vessel can fail through either shell instability or axisymmetric collapse or as will be shown later in the present text, by a combination of these two modes of failure.

Earlier work by Esslinger and Geier (1974) and also by Malik *et al.* (1979) were only concerned with the elastic instability of geometrically perfect vessels. From the theory of Esslinger and Geier and according to Rajagopalan (1993), the former authors quoted the following semiempirical formula to predict the elastic instability of varying thickness circular cylinders under hydrostatic pressure:

$$\frac{L}{P_{cr}} = \sum_{i=1}^{i=N} \frac{L_i}{P_i} \tag{1}$$

L = the entire length of the vessel between supports
P_{cr} = theoretical elastic buckling pressure based on the von Mises theory
P_i = theoretical buckling pressure of the ith bay of the vessel, assuming that it is of length L and of thickness t_i
L_i = length of the element 'i'

The material properties of the vessels were found by experiment to be as follows:

Yield stress = σ_{yp} = 263 MPa
Young's modulus = E = 190 GPa
Nominal Peak stress = σ_{UTS} = 379 MPa

Assumed Poisson's ratio = v = 0.3
The initial out-of-circularites 'e'of the models were measured and found to be as follows:

VT1 At the middle of vessel, e = 0.0181 mm

VT2 At the middle of the top section (where the vessel buckled), e = 0.0157 mm
At the middle of the bottom section (where the vessel started to buckle), e = 0.0152 mm
VT3 In the middle of the thin section (where the vessel buckled), e = 0.0208 mm

These initial out-of-circularities were measured on the external surfaces of the vessels and it can be seen that they were small. That is, their eccentricity to thickness ratios varied from about 1/100 to 1/70.

The buckling pressures P_i were calculated form the von Mises formula (1929) for uniform thickness circular cylinders, assuming that they were simply supported at their ends and subjected to uniform external pressure. This formula which is listed below, has also been published by Ross (1990), together with a computer program to implement it.

P_{cr} = von Mises buckling pressue

$$= \frac{E(t/a)}{[n^2 - 1 + 0.5(\pi a/L)^2]} \left\{ \frac{1}{n^2 L/(\pi a)^2 + 1]^2} + \frac{t^2}{12a^2(1-v^2)} \left[n^2 - 1 + \left(\frac{\pi a}{L}\right)^2 \right]^2 \right\} \tag{2}$$

where

E = Young's modulus of elasticity
a = mean radius of cylinder
t = wall thickness of cylinder
n = number of circumferential waves the vessel buckles into

The main deficiency of the theory of Esslinger & Geier is that it does not take into account the detrimental effects of initial out-of-circularity, nor that the vessels can fail through inelastic instability. Both of these effects can cause the predicted buckling pressures to be considerably smaller than the theories of von Mises, Esslinger and Geier. The paper by Malik *et al.* was also aimed at perfect vessels that failed by elastic instability. Additionally, it was difficult to interpret the experimental results of Malik *et al*; because the tops of their vessels were not secured firmly and this led to some difficulty in determining the exact experimentally observed buckling pressures of some of their vessels.

Hence, because there appears to be a shortage of experimentally observed buckling pressures for varying thickness circular cylinders under external hydrostatic pressure, especially for those that failed inelastically, the present investigation was conducted.

In the present paper, a report will be made of a theoretical and an experimental investigation of three varying thickness circular cylinders that were tested to destruction under external hydrostatic pressure.

2. Apparatus

Three models were accurately machined from a solid billet of EN1A mild steel. First of all, the internal surface of each vessel was bored out and then each model was placed on a previously machined, mandrel, where the outer surface was carefully machined. Thus, the step variation in wall thickness was on the outer surface of each vessel.

2.1. The models VT1, VT2 & VT3

Details of the geometrical properties of each vessel are shown in Figs. 4 to 6, where the dimensions are in mm. The models were named, VT1, VT2 and VT3 and a photograph of the three models is shown in Fig. 7, where P_i = the von Mises buckling pressure for the element of the varying tickness cylinder which is of length 'L_i' and thickness't_i'.

Additionally, as the vessels were of varying thickness, it will be necessary to suggest a new method of calculating the thinness ratio 'λ' (Windenburg & Trilling 1934).

$$\lambda = ((L/2a)^2/(t/2a)^3)^{0.25}\sqrt{(\sigma_{yp}/E)} \tag{3}$$

σ_{yp}= yield stress

The symbol 'λ' of Eq. (3) represents a thinness ratio for circular cylinders, when Windenburg and Trilling obtained 'λ' based on the ability of a thin-walled circular to resist both instability and axisymmetric deformation. Thus 'λ' is related to both the geometrical and material properties of the vessel. 'λ' can be regarded as being the cylindrical shells' equivalent of the well-known slenderness ratio for struts, except that 'λ' is also related to both the yield stress of the material and Young's modulus.

It should be emphasised that because the vessels buckled under external hydrostatic pressure,

many vessels will buckle at pressures that are considerably less than those predicted by elastic theory for perfect vessels. It is because of this that Ross (1990) introduced a plastic knockdown factor (PKD) based on thinness ratio of Windenburg & Trilling; this plastic knockdown factor is used as shown in Eq. (4)

$$P(\text{predicted}) = P_{cr}/(\text{PKD}) \tag{4}$$

where

P (predicted) = predicted buckling pressure
P_{cr} = theoretical elastic instability buckling pressure for perfect vessels
PKD = plastic knockdown factor for uniform thickness cylinders, obtained from the semiempirical chart of Ross (1990)

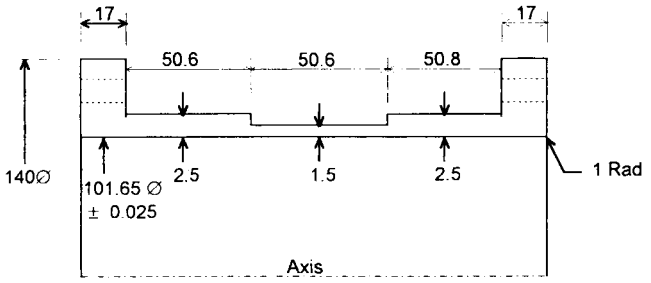

Fig. 4 Geometrical details of VT1

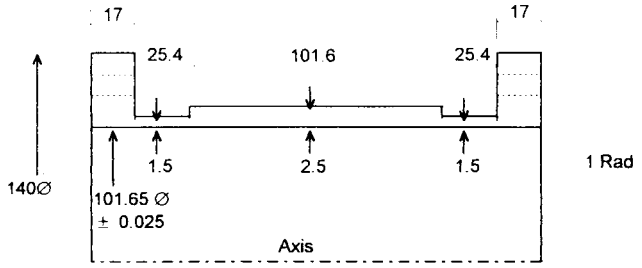

Fig. 5 Geometrical details of VT2

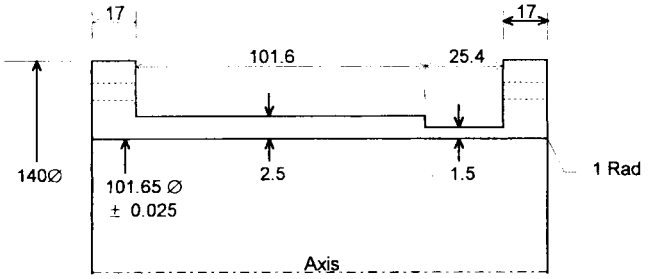

Fig. 6 Geometrical details of VT3

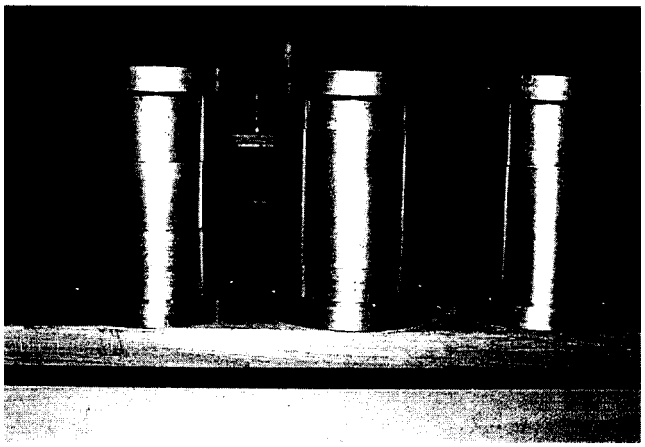

Fig. 7 Models VT1, VT2, & VT3

The present authors suggest that for a varying thickness circular cylinder 'λ' is calculated by Eq. (5)

$$\frac{L}{\lambda} = \sum_{i=1}^{N} (L_i/\lambda_i) \tag{5}$$

where λ_i is calculated for a circular cylindrical shell element of length 'L_i' and of thickness 't_i'. The original formula for 'λ' is given by Eq. (3)

2.2. The test tank

The test tank is shown schematically in Fig. 8, where it can be seen that the models were hung vertically from their top to eliminate secondary bending stresses.

The external hydrostatic pressure was applied by a hand-operated hydraulic pump so that line losses were negligible. Water was used as the pressure raising fluid and because of this, all the electrical resistance strain gauges were attached to the internal surfaces of the models, so that the water proofing of strain gauges was avoided.

3. Experimental procedure

Fifteen electrical resistance strain gauges were attached to VT1 and VT2 and nineteen strain gauges were attached to model VT3, as shown schematically in Figs. 9 to 11.

It can be seen from Figs. 9 to 11 that ten circumferential strain gauges were attached to the midspans of the thinner sections for VT1 & VT3 and 10 gauges to the mid-span of the thicker section for VT2. It was expected that the vessels would buckle in these positions and these strain gauges were required to observe the non-linear behaviour during buckling. In some cases, a teestacked pair of strain gauges was used in certain areas, so that the two principal stresses at those points could be observed. It was intended to compare these experimentally observed stresses with the theory of Ross (1970). A computer program, based on this theory has been published by Ross (1990).

3.1. The experimental tests

The external hydrostatic pressure for each of the three experimental tests was first increased to 34.47 bar and the strain gauges read. The process was repeated at pressures of 51.71 bar and 68.95 bar and then the hydrostatic pressure was decreased to zero. The strain gauges readings were then read at zero pressure to test for any drifting, but all the strain gauges behaved quite satisfactorily. The hydrostatic pressure for each of the three vessels was then increased gradually in increaments of 34.47 bar and the strain gauges read. When the strain gauges started to behave non-linearly, the increments of pressure were made smaller and smaller, until failure occurred.

The model VT1 collapsed as expected throgh inelastic shell instability at the mid-span of the

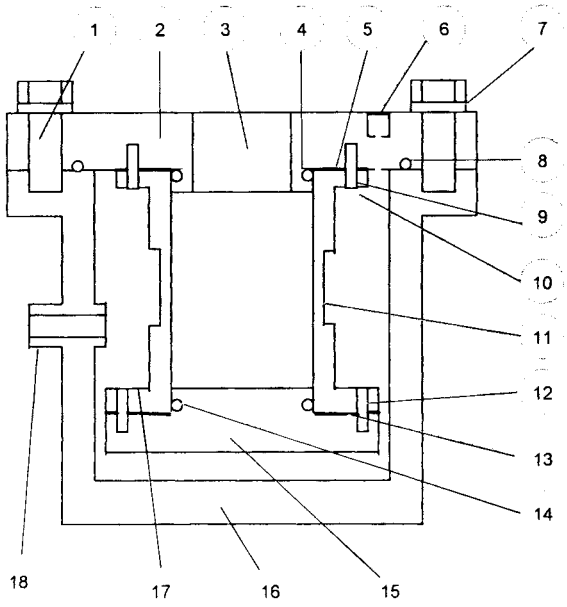

1 Large bolts
2 Top plate
3 Hole in middle of top plate
4 O-ring seal
5 Gasket
6 Hole to evacuate air from tank (threaded at top for bolt to screw on)
7 Washer
8 O-ring seal
9 Small bolt
10 Small washer
11 Vessel V T 1
12 Small bolt
13 Gasket
14 O-ring seal
15 End plate
16 Tank
17 Small washer
18 Hole in side of tank for water to be pumped in (threaded around the outside).

Fig. 8 The test tank and a model

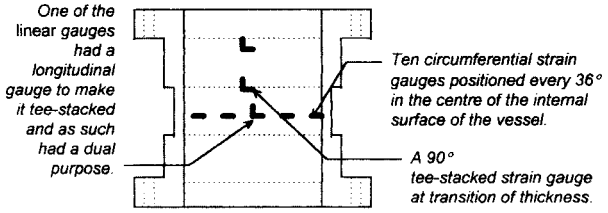

Fig. 9 Strain gauge positions for VT1

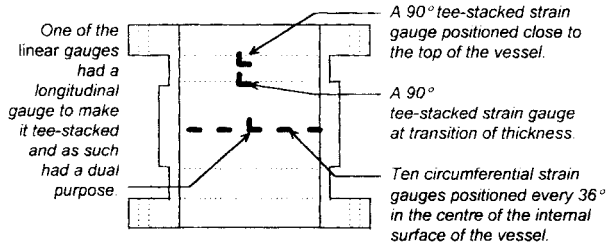

Fig. 10 Strain gauge positions for VT2

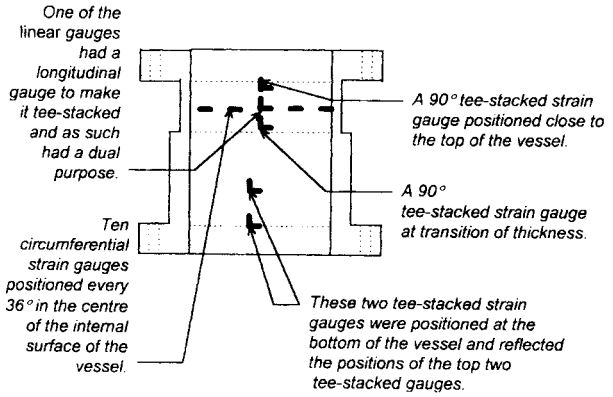

Fig. 11 Strain gauge positions for VT3

vessel, in its thinner region. For this mode of failure, the hoop stresses at mid-bay reached yield, causing some plastic axisymmetric deformation. The effect of this was to cause the circumferential tangential modulus to become a small fraction of the Young's modulus of elasticity, thereby triggering of plastic shell instability. It was expected that model VT2 would also collapse at midspan, because although the model was thicker here, the meridional length of the thicker section was four times larger than the meridional lengths of the two thinner sections. However, the model collapsed in the top thinner section by a mode of failure which was a combination of shell instability and axisymmetric collapse. Later inspection of the collapsed vessel showed that the bottom thinner section of model VT2 had started to collapse axisymmetrically, triggering off plastic shell instability, as described above. The model VT3 collapsed as expected through inelastic shell instability in the thinner section. A photograph of the collapsed models is shown in Fig. 12 and the experimentally obtained buckling pressures are given in Table 1.

These experimentally obtained buckilng pressures where quite violent with a rapid fall in the value of the applied pressure. This was quite unlike plastic axisymmetric collapse, which was much more gentle and which required some time and effort to cause the three hinge mechanism described earlier.

3.2. Strain gauge recordings

The strain gauges recordings for each of the cicumferential sets of gauges for models VT1, VT2 and VT3 are shown in Figs. 13 to 15. These figures show how the magnitudes of circumferential strain grow with increasing values of exteternal hydrostatic pressure and in all cases, the vessels failed plastically.

Table 1 Experimental collapse pressures (bar) of VT1, VT2 and VT3

Model	Buckling pressure (P_{exp})	Region of failure
VT1	103.42	Mid-span
VT2	123.07	Top thinner section
VT3	99.97	Thinner section

Fig. 12 Collapsed models VT1, VT2 and VT3

4. Theoretical analyses

Three different types of theoretical analyses were carried out; one was a linear elastic axisymmetric deformation analysis while another was a non-linear non-symmetrical bifurcation buckling analysis, based on plastic knockdown. A third analysis was based on a finite element analysis involving geometrical and material non-linearity.

The purpose of the first of these analyses was to study the distribution of axisymmetric stress along a meridian for varying thickness circular cylinders. The other analyses were to obtain a method of calculating the inelastic buckling pressures for varying thickness circular cylinders under hydrostatic pressure.

4.1. Linear axisymmetric deformation analysis

This theory was based on the axisymmetric slope deflection analysis for shells (Ross 1970). The theory solved the shell differential equation of Wilson (1956) by the method of Salerno and Pulos (1951), but allowed for non-symmetric deformation about mid-span due to the vessel being of varying thickness. The method of anaysis will not be described here, as it is adequately described elsewhere (Ross 1990).

4.2. Inelastic buckling analyses

The problem with the theory of Esslinger & Geier was that when P_i was calculated, the entire length of the vessel was used for all elements. The present authors thought that this process seemed

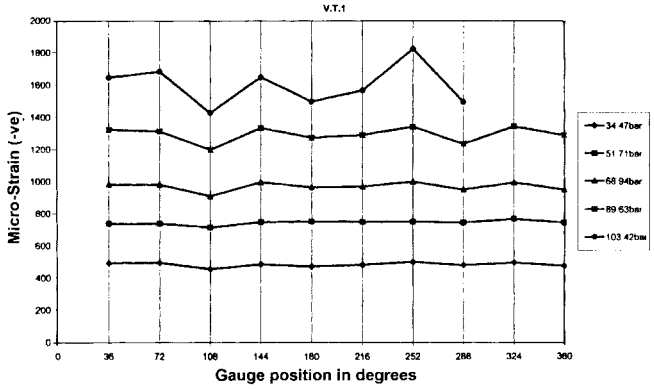

Fig. 13 Circumferential strain distribution for VT1 at different pressures

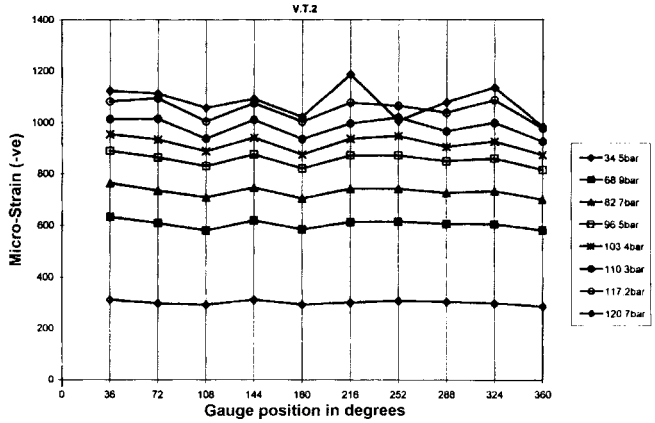

Fig. 14 Circumferential strain distribution for VT2 at different pressures

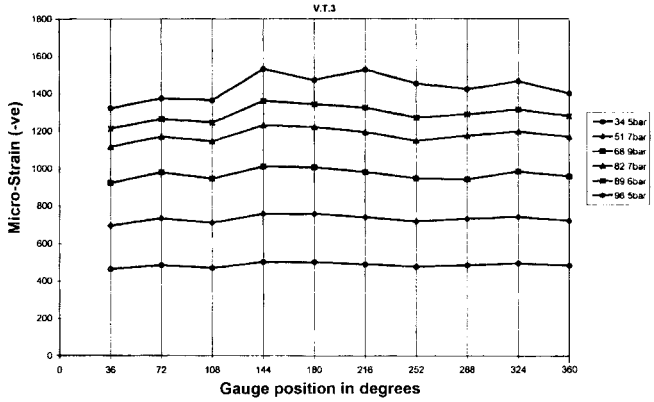

Fig. 15 Circumferential strain distribution for VT3 at different pressures

somewhat illogical, as the length of each section of the varying thickness cylinder could be different. Because of this, the present authors suggested the following formula:

$$\frac{L}{P_{cr}} = \sum_{i=1}^{i=N} (L_i/P_i) \tag{6}$$

For the sake of continuity, with the Esslinger & Geier method, an additional calculation for 'λ' will be made, where like Esslinger & Geier, 'L_i' will be made to be the entire length of the vessel. Additionally inelastic buckling solutions will be made using the plastic knockdown factor together with finite element truncated conical shell element of Ross (1990).

5. Comparisons between experiment and theory

Two separate analyses will be made; one of these will involve a linear elastic axisymmetric deformation analysis and the other will be in determining the inelastic buckling pressures of these vessels by five different methods.

5.1. Linear axisymmetric stress distrbutions

The theoretical axisymmetric stress distributions along a longitudinal generator, under a uniform external pressure of 34.47 bar, are shown in Figs. 16 to 18. In these cases, comparisons between experiment and theory was not possible as no strain gauges were attached to the external surfaces of the models. However, as it is possible that these stresses can be larger than their internal counterparts, they are presented here.
x = distance measured from an end in mm

5.2. Inelastic buckling

In this case, five analyses will be carried out. One analysis will be based on the theory of Esslinger and Geier (1974) and two solutions will be based on the finite element solution of Ross (1990). One of the finite element theories will calculate 'λ' by the concept of Esslinger & Geier while the other theory will calculate 'λ' according to Eq. (4). A fourth inelastic theory will be based on the modified version of Esslinger & Geier, as suggested by the present authors and by using Eqs. (2) and (4). A fifth analysis will be by using the finite element method, allowing for geometrical and material non-linearity, as described in Secton 5.2.1. This theory is similar to that of Bushnell (1976).

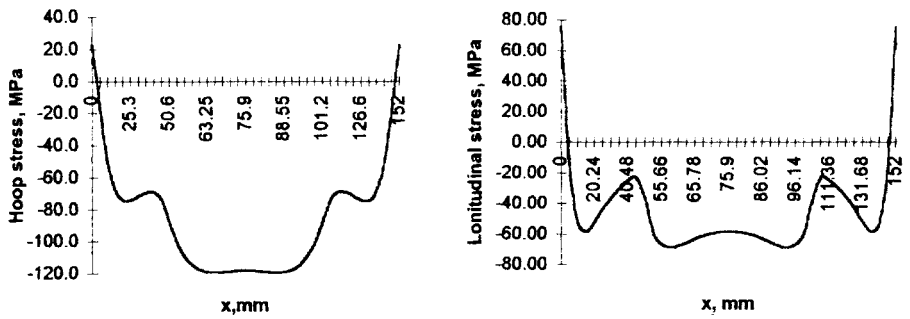

Fig. 16 Hoop and longitudinal stress distributions for VT1 (external surface)

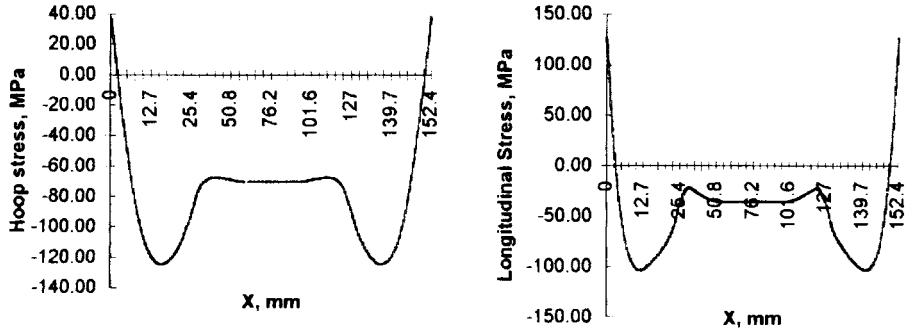

Fig. 17 Hoop and longitudinal stress distributions for VT2 (external surface)

Table 2 shows the results for the two theories based on the Esslinger & Geier concept, where

P_{cr} (1)= the theoretical elastic buckling pressure as predicted by Esslinger & Geier
P_{cr} (2)= the theoretical elastic buckling pressure as predicted by the finite element method
λ (1) = the thinness ratio as calculated by the concept of Esslinger and Geier
PKD = plastic knockdown factor (Ross *et al.* 1995)
P (1) = P_{cr}(1)/PKD = predicted inelastic buckling pressure by the concept of Esslinger & Geier
P (2) = P_{cr}(2)/PKD = predicted inelastic buckling pressure by FEM (method 1)
P_{exp} = experimentally obtained buckling pressures

Table 3 shows the buckling pressures for the two theories based on the approach suggested in the present paper;

where

P_{cr} (3)= the theoretical buckling pressure predicted by the finite element method.
P_{cr} (4) = the theoretical buckling pressure based on the modified theory of Esslinger & Geier
λ (2) = the thinness ratio as calculated by the present approach (see Eq. 5)
PKD = plastic knockdown factor (Ross *et al.* 1995)
P (3) = P_{cr} (3)/PKD predicted
P (4) = P_{cr} (4)/PKD buckling pressures

Table 2 Buckling pressure (bar) by method (1)

Model	P_{cr} (1)	P_{cr} (2)	λ (1)	PKD	P(1)	P(2)	P_{exp}
VT1	170.6	211.3	0.835	2	85.31	105.7	103.42
VT2	170.0	383.7	0.836	2	85.01	191.9	123.07
VT3	170.0	280.3	0.836	2	85.01	140.2	99.97

Table 3 Buckling pressure (bar) by method (2)

Model	P_{cr} (3)	P_{cr} (4)	λ (2)	PKD	P(3)	P(4)	P_{exp}
VT1	211.3	556.0	0.482	5.0	42.3	111.2	103.42
VT2	383.7	521.9	0.544	4.0	95.9	130.5	123.07
VT3	280.3	388.3	0.618	3.4	82.4	114.2	99.97

P_{exp} = experimental buckling pressure

From Tables 2 and 3, it can be seen that the inelastic theory, based on the modified method of Esslinger & Geier gives very good results; the errors being between + 6% to +12%. The inelastic theory based on the original concept of Esslinger & Geier gives poor results, the errors by method (1) being between +2.2% to +56% and the errors by method (2) being −18% to −59%. Even more encouraging about the modified theory of Esslinger & Geier is that its errors had a small standard deviation.

5.2.1. Non-linear finite element solution

Unlike the previous two finite element solutions, which were based on dividing a theoretical linear solution by previously obtained semi-empirical plastic knockdown factors, the finite element solution described here allows for material and geometrical non-linearity. In this case, the axisymmetric thin-walled conical shell element (Ross, 1990) was used. The method of analysis allows for both geometrical and material non-linearity and is based on a step-by-step incremental procedure, which is now described with the aid of Table 4.

The incremental non-linear method is to load each vessel in increments of pressure, namely $\{\delta q_i^0\}$, and to observe the theoretical behaviour of the vessel due to each increment of pressure. The process therefore, is that at the end of the first stage, to calculate the displacements $\{\delta u^0_i\}$ and the stresses, due to the first increment in pressure, and to update the geometry of the vessel due to this load. Additionally, if any element in a vessel became plastic, according to the Hencky-von Mises theory of yield, to change the value of the Young's modulus for that element. It was assumed that if the von Mises stress reached first yield for any element, its Young's modulus became 1/5th of its elastic Young's modulus, and that when the von Mises stress reached 1.1 of the yield stress, the Young's modulus became 1/100th of its elastic Young's modulus. The process was repeated for the other stages, where the displacements and stresses were superimposed at the end of each stage. Each vessel was assumed to be fixed at one end, and clamped at the other end.

Where

$[K]= [K_0] + [K_G]$
$[K]$= Stiffness matrix
$[K_0]$= a stiffness matrix (If the material properties of the element are constant, then this matrix is the

Table 4 Incremental non-linear method

Step	$\{\delta q^0\}$	Stiffness matrix	$\{\delta u^0\}$	Displacements
1	$\{\delta q_1{}^0\}$	$[K_0{}^0(0)]+[K_G{}^0(0)]$	$\{\delta u_1{}^0\}$	$(u_1{}^0\} = (\delta u_1{}^0\}$
2	$\{\delta q_2{}^0\}$	$[K_0{}^0\{u_1{}^0\})]+[K^0{}_G(u_1{}^0)]$	$\{\delta u_2{}^0\}$	$\{u_2{}^0\} = \{u_1{}^0\}+\{\delta u_2{}^0\}$
3	$\{\delta q_3{}^0\}$	$[K_0(u_2{}^0)]+[K_G{}^0(u_2{}^0)]$	$\{\delta u_3{}^0\}$	$\{u_3{}^0\} = \{u_2{}^0\}+\{\delta u_3{}^0\}$
.				
.				
.				
.				
n	$\{\delta q_n{}^0\}$	$[K_0{}^0\{u_{n-1}{}^0\}]+[K_G{}^0(u_{n-1}{}^0)]$	$\{\delta u_n{}^0\}$	$\{u_n{}^0\} = \{u^0{}_{n-1}\}+\{\delta u_n{}^0\}$
Σ	$\{q_n{}^0\}$			$\{u_n{}^0\}$

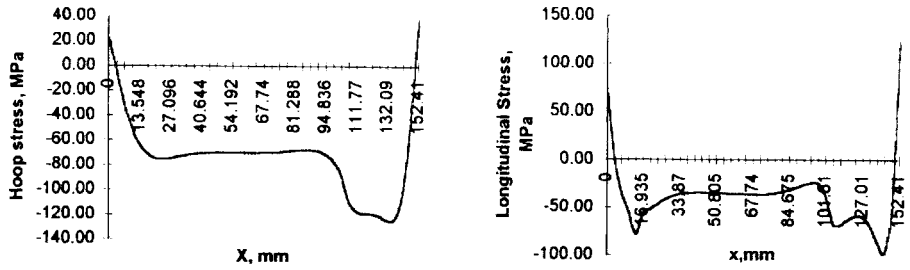

Fig. 18 Hoop and longitudinal stress distributions for VT3 (external surface)

usual stiffness matrix)

$[K_G]$= the geometrical stiffness matrix which depends on the internal forces in the element. This is also known as the *initial stress-stiffness matrix.*

This then leads on to the following, which shows the equation step by step.

$$[K] = [K(u_i^0)] + K_G(u_i)]$$

Where

$[K]$ = The stiffness matrix
$[K(u_i^0)]$ = The stiffness matrix at the ith step
$[K_G(u_i^0)]$= The geometrical stiffness matrix at the ith step
$\{\delta q^0\}$ = Incremental load

From the theoretical results obtained from the non-linear finite element computer program, the external pressures were plotted against the end axial deflection, for each of the three vessels. On each of the three graphs the experimental buckling pressures were also plotted, as shown in Figs. 25 to 27.

Comparisons between theory and experiment are shown in Figs. 19 to 24 for the internal surfaces of these vessels, under an external hydrostatic pressure of 34.47 bar.

x = distance measured from an end in mm

From Figs. 19 to 24, it can be seen that good agreement was found between experiment and theory except at the ends. It appears that the main reason for the discrepancy between experiment and theory of the ends was that the ends of the vessels were not 100% fixed, as assumed in the theory of Ross. That is, there was some elastic relaxation at the ends of the vessels.

The theory has shown that in all cases, the vessels collapsed in the regions of highest hoop stress. In fact it can be seen that despite the fact that the thinner sections had much shorter meridional lengths than the thicker sections, the largest hoop stresses lay in these thinner sections. In fact, in all three cases, the hoop stresses in the thinner sections were some 50% larger than the hoop stresses in the thicker sections. Thus it can be concluded that for these vessels, a linear axisymmetric deformation analysis can serve as a useful method of analysis in addition to an inelastic buckling analysis.

The figures show that there was good agreement between the theoretically obtained buckling pressures with the experimentally obtained buckling pressures; the numerical values are shown in Table 5.

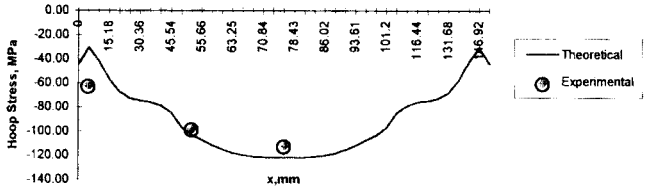

Fig. 19 Hoop stress distributions for VT1 (internal)

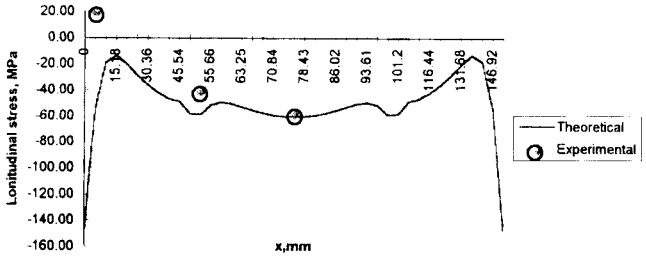

Fig. 20 Longitudinal stress distribution for VT1 (internal)

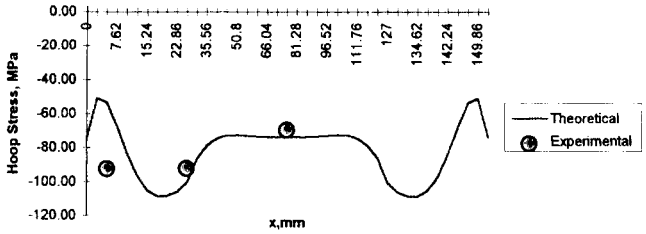

Fig. 21 Hoop stress distributions for VT2 (internal)

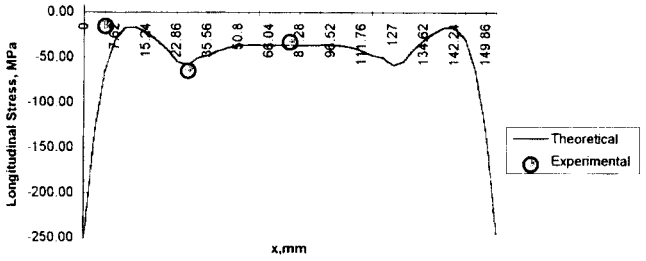

Fig. 22 Longitudinal stress distribution for VT2 (internal)

6. Conclusions

The experimental results have shown that all three vessels collapsed by inelastic instability. Models VT1 and VT3 collapsed by inelastic non-symmetric bifurcation buckling, while model VT2 collapsed by a mixed mode of inelastic non-symmetric bifurcation buckling and plastic axisymmetric deformation. This latter observation appears to indicate that there is a link between inelastic non-symmetric bifurcation buckling and plastic axisymmetric deformation.

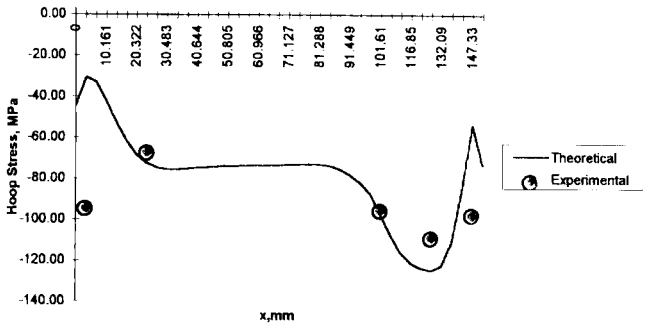

Fig. 23 Hoop stress distributions for VT3 (internal)

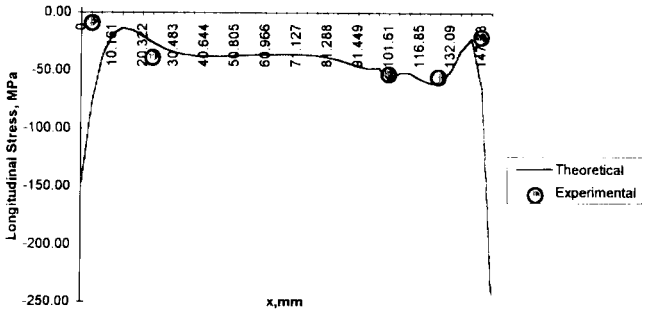

Fig. 24 Longitudinal stress distribution for VT3 (internal)

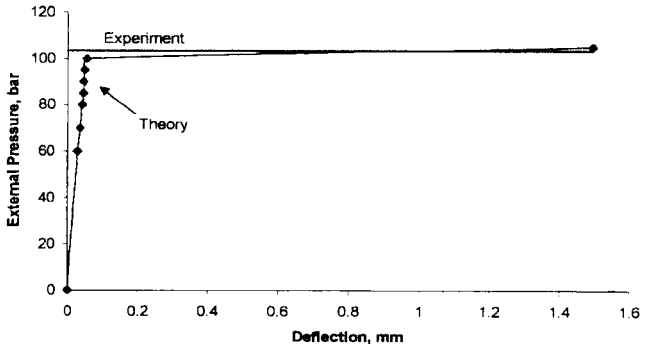

Fig. 25 Experimental buckling pressure for V.T.1., as a comparison with the non-linear finite element solution

It appears that in all three cases, the maximum hoop stress reached yield and this caused the circumferential tangent moduli to become much smaller than the Young's modulus, thereby triggering catastrophic collapse. The modified theory of Esslinger & Geier, which allowed for inelastic buckling, gave very good results, while the two finite element solutions based on dividing theoretically obtained linearly elastic buckling pressures by experimentally obtained plastic knockdown factors gave poor results.

The non-linear finite element solution gave excellent results. The linear elastic theory for axisymmetric stress predictions along the meridional length of each vessel gave good results and

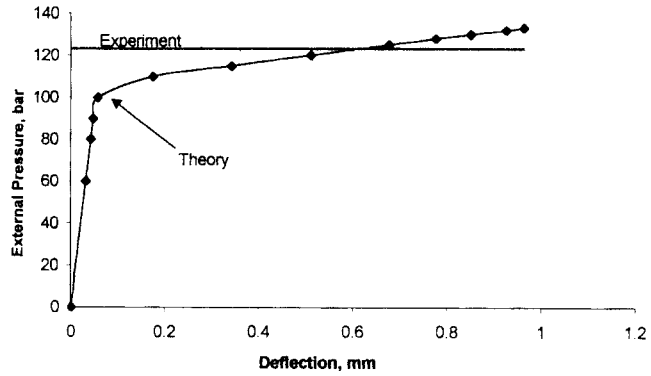

Fig. 26 Experimental buckling pressure for V.T.2., as a comparison with the non-linear finite element solution

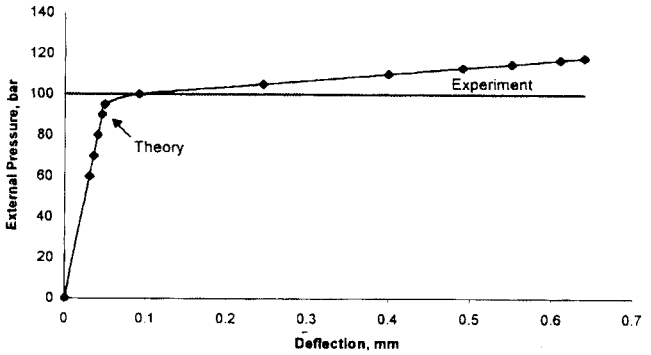

Fig. 27 Experimental buckling pressure for V.T.3., as a comparison with the non-linear finite element solution

Table 5 Comparison between the non-linear finite element solution and experiment

	Non-linear finite element buckling pressure (bar)	Experimental buckling pressure (bar)
V.T.1	104	103.42
V.T.2	115	123.07
V.T.3	100	99.97

showed that collapse occurred in regions of high hoop stress.

Acknowledgements

The authors would like to thank Grant Waterman and Phil Bennett for their assistance. Their thanks are extended to Dr. Monty Bedford for encouraging this work. Lastly but not leastly, the authors would like to thank Miss Katrina Corby for the care and devotion she showed in typing this manuscript.

References

Bushnell, D. (1976), "BOSOR program for buckling of elastic-plastic complex shells of revolution, including large deflection and creep" *Computers and Structures*, **6**, 221-239.

Esslinger, M. and Geier, B. (1974), "Buckling loads of thin-walled circular cylinders with axisymmetric irregularities", Paper 36, *Int. Conf. on 'Steel Plated Structures'*, London.

Malik, Z. Morton, J. and Ruiz, C. (1979), "An experimental investigation into the buckling of cylindrical shells of variable wall thickness under Radial external pressure", *Experimental Mechanics*, **36**, 87-92.

Rajagopalan, K. (1993), *Finite Element Buckling Analysis of Stiffened Cylindeical Shells.*

Ross, C.T.F. (1990), *Pressure Vessels under External Pressure*, Chapman and Hall.

Ross, C.T.F. (1970), "Axisymmetric deformation of a varying strength ring-stiffened cylinder under lateral and axial pressure", *Trans RINA*, **112**, 113-117.

Ross, C.T.F., Haynes, P., Seers, A. and Johns, T. (1995), "Plastic collapse of thin-walled ring-stiffened circular cylinders under uniform external pressure", *Int. ASME Conference on Structural Dynamics & Vibration*, PD-Colito, Houston, Texas.

Salerno, V.L. and Pulos, J.G. (1951), "Stress distribution in a circular cylindrical shell under hydrostatic pressure supported by equally spaced circular ring frames", Polytechnic Institute of Brooklyn Report, No 171-A, June.

Von Mises, R. (1929), "Der Kritische Aussendruck Fur Allsiets Belastete Zylindrische Rohre, Fest Zum 70", Geburststag von Prof. A Stodola, Zurich, 418-30 (Also US DTMB Translation Report NO. 366, 1936).

Wilson, L.B. (1956), "The deformation under uniform pressure of a circular cylindrical shell supported by equally spaced ring frames", NCRE Report No 337B, December.

Windenburg, D.F. and Trilling, C. (1934), "Collapse by instability of thin cylindrical shells under external pressure", *Trans. ASME*, **11**, 819-825.